RESEARCH ARTICLE

A Feedback Loop of LINC00665 and the Wnt Signaling Pathway Expedites Osteosarcoma Cell Proliferation, Invasion, and Epithelial-Mesenchymal Transition

Jinyu Bai, PhD[1], Xiao Zhang, PhD[2], Fengxian Jiang, BD[1], Huajian Shan, PhD[1], Xiang Gao, PhD[1], Lin Bo, PhD[3], Yingzi Zhang, PhD[1]

Department of [1]Orthopaedics, [2]Traditional Chinese Medicine Orthopaedics and [3]Rheumatology, the Second Affiliated Hospital of Soochow University, Suzhou, China

Objectives: Osteosarcoma (OS) is a malignant tumor with frequent occurrence among teenagers. Long non-coding RNAs (lncRNAs) play pro-cancer roles in many tumors. The purpose of this study was to figure out the functional role of a novel lncRNA long intergenic non-protein coding RNA 665 (LINC00665) in OS by observing the OS cell behaviors.

Methods: Quantitative reverse transcription polymerase chain reaction (RT-qPCR) was used to analyze LINC00665 expression in OS cells. Cell function assays assessed the impacts of LINC00665 on OS cell phenotype. Immunofluorescence and western blot analyzed the function of LINC00665 on epithelial-mesenchymal transition (EMT) in OS. Moreover, mechanistic assays analyzed the downstream mechanism of LINC00665 in OS cells.

Results: LINC00665 was significantly up-regulated in OS cells. LINC00665 silence facilitated OS cell proliferation, migration, invasion, and EMT while inhibiting cell apoptosis. Mechanically, LINC00665 acted as a competing endogenous RNA (ceRNA) to sponge miR-1249-5p and thereby modulated Wnt family member 2B (WNT2B) to activate Wnt pathway. Wnt pathway activated LINC00665 expression transcriptionally.

Conclusions: Our study uncovered the cancer-promoting role of LINC00665 in OS, and the feedback loop of LINC00665/miR-1249-5p/WNT2B/Wnt might be a potential target for OS treatment.

Key words: LINC00665; miR-1249-5p; Osteosarcoma; WNT2B

Introduction

Osteosarcoma (OS) is a primary malignant bone tumor, which often happens in adolescence.[1] It is developed from bone mesenchymal cells and the characteristics of OS are rapid growth, high degree of malignancy, easy recurrence, and remote metastasis.[2] Globally, the incidence of OS is about 1–3 cases among 1,000,000 every year, and the highest-risk populations are children and adolescents.[3] In addition to higher risks of infection induced by chemotherapy-induced immunosuppression, adolescents accepting limb salvage with endoprosthetic reconstruction might suffer from prosthetic loosening and limb length discrepancy over time, which require additional surgeries.[4] With the advances in therapeutic strategies including combinatorial chemotherapy and radiotherapy, the 5-year survival rate of pediatric OS patients is 61.6% globally.[5,6] Recently, increasing evidence has suggested

Address for correspondence Lin Bo, Department of Rheumatology, the Second Affiliated Hospital of Soochow University, No. 1055, Sanxiang Road, Gusu District, Suzhou, 215004, Jiangsu, China; Email: linbilugx9@163.com
Yingzi Zhang, Department of Orthopedics, the Second Affiliated Hospital of Soochow University, No. 1055, Sanxiang Road, Gusu District, Suzhou, 215004, Jiangsu, China; Email: zhangyz@suda.edu.cn
Jinyu Bai, Xiao Zhang and Fengxian Jiang are co-first authors.
Received 23 January 2022; accepted 6 September 2022

that molecular mechanisms play significant roles in the development and progression of OS.[7] For instance, PTEN/PI3K/AKT/mTOR pathway has been suggested to exert anti-tumor influence in OS,[8] and TRIM7/BRMS2 axis regulated by METTL3/YTHDF2 through m^6A modification has been claimed to play a key role in OS metastasis.[9] Therefore, identifying the potential moleculars and detailed mechanisms is essential for the exploration of effective treatment for OS patients.

Abnormally expressed long non-coding RNAs (lncRNAs) engage in cell apoptosis and other multiple physiological processes.[10] Accumulating evidence has demonstrated that lncRNAs can exert tumor-promoting or tumor-suppressing influence in the tumorigenesis and development of OS.[11] LncRNA H19 impedes OS cell migration and invasion through NF-κB pathway.[12] GAS5 functions as an antitumorigenic role in OS via sponging miR-203a to regulate TIMP2.[13] Long intergenic non-protein coding RNA 665 (LINC00665) has been found to display abnormally high expression in prostate cancer[14] and breast cancer.[15] Moreover, LINC00665 facilitates multiple myeloma cell proliferation via sponging miR-214-3p to regulate PSMD10 and ASF1B expression.[16] LINC00665 facilitates the hepatocellular carcinoma via activating PKR/NF-κB pathway.[17] However, the role of LINC00665 in OS remains largely obscure.

Wnt signaling pathway is an active regulator in growth and development throughout the animal kingdom.[18,19] The activation/inactivation of the Wnt signaling pathway is greatly implicated in the occurrence and progression of multiple cancers, including OS.[20] Wnt family member 2B (WNT2B) is a subtype of Wnt protein family.[21] Mounting studies have uncovered the involvement of WNT2B-mediated Wnt signaling pathway in the progression of many cancers, including OS.[22] Additionally, Wnt pathway has been reported to activate the transcription of lncRNAs in cancers.[23]

Herein, we concentrated on the role of LINC00665 in OS cells. We also discussed the regulatory mechanism of LINC00665 in OS cells and unveiled the interaction between LINC00665 and the Wnt signaling pathway. With all these efforts, a novel molecular mechanism critical to the modulation of OS cell malignant behaviors could be explicitly clarified, and a more thorough understanding of OS at a molecular level could be gained. Hopefully, effective biomarkers targeting OS could be applied in OS treatment in the future based on our study.

Methods

Cell Culture

American Type Culture Collection supplied OS cells (U2OS, SAOS-2, MG-63 and 143B) and human fetal osteoblasts (hFOB). U2OS and SAOS-2 cells were cultured in McCoy's 5a Medium (Gibco). MG-63 and 143B cells were cultured in Eagle's Minimum Essential Medium (Gibco). hFOB cells were cultured in Dulbecco's Modified Eagle Medium (Gibco). All cell cultures were added with 10% fetal bovine serum (FBS) and 1% penicillin–streptomycin in a humid incubator. OS cells were cultured at 37°C with 5% CO_2, while hFOB cells were cultured at 34°C with 5% CO_2.

Cell Transfection

Three specific short hairpin RNAs (shRNAs) of LINC00665 and sh-NC (negative control), miR-1249-5p mimics and NC mimics, miR-1249-5p inhibitor and NC inhibitor as well as pcDNA-LINC00665, pcDNA-WNT2B, and pcDNA were obtained from GenePharma. Lipofectamine™ 3000 Transfection Reagent (Thermo Scientific) was used for cell transfection for 48 h. Then, cells with stable transfection were selected by puromycin (2 μg/ml) for 2 weeks. The sequences of the above-mentioned overexpression and knockdown plasmids were provided in Supplementary file 1.

Quantitative Reverse Transcription Polymerase Chain Reaction

Total RNA from cells (3×10^7) was extracted and purified with Trizol reagent (Invitrogen) according to manufacturer's instruction. Then complementary DNA (cDNA) was synthesized using RevertAid First Strand cDNA Synthesis Kit (Thermo Scientific) based on provider's suggestions, followed by qPCR via GoTaq qPCR Master Mix (Promega). $2^{-\Delta\Delta Ct}$ method was used to calculate the expression levels of genes relative to glyceraldehyde-3-phosphate dehydrogenase (GAPDH) and U6 respectively.

Cell Counting Kit-8

Transfected cells during the logarithmic growth were grown in 96-well plates (2000 cells per well). Then 10 μl CCK-8 solutions (Beyotime) were added into each cell for incubation at 37°C for 1 h. The absorbance was detected at 450 nm using a microplate reader (Molecular Devices).

5-Ethynyl-2′-deoxyuridine

Transfected cells (1×10^5) were centrifuged and plated into 12-well plates. Then 10 μM EdU working solutions (Beyotime) were added into each cell for incubation at 37°C for 2 h. Then cells were treated with 4% paraformaldehyde (Sangon) and phosphate-buffered saline (PBS), and then permeated using 0.3% Triton X-100 (Sangon). Next, each cell was added 50 μl Click reaction solution for 30 min incubation in the dark. Finally, 4′, 6-diamidino-2-phenylindole (DAPI) was used for cell counterstaining and the images were observed using a fluorescence microscope.

Colony Formation

Transfected cells were seeded into six-well plates with the density of 500 cells for incubation. After 1 week, the cultivation was stopped when the visible clones were appeared in culture dish. Then cells were fixed with 4% paraformaldehyde and stained with 0.3% crystal violet (Beyotime), followed by counting the number of colonies.

Caspase-3 Activity

The activity of caspase-3 in cells (2.5×10^6) was determined by Beyotime C1115 Caspase 3 Activity Assay Kit in line with instructions. The cell protein extracts were incubated with

caspase-3 buffer for 4 h. Then the absorbance at 405 nm was detected by spectrophotometer.

Terminal-Deoxynucleoitidyl Transferase Mediated Nick End Labeling

Transfected cells (2.5×10^5) were grown in 12-well sterile plates, and then centrifuged for 5 min. Next, the cells were re-suspended and washed by PBS, followed by the treatment of 4% paraformaldehyde and 0.3% Triton X-100. Finally, 50 μl TUNEL liquid (Beyotime) was added to cells for 60 min incubation. DAPI was used for cell counterstaining, and the images were observed using a fluorescence microscope at 20 × 10 magnification.

Wound Healing

Cells in the logarithmic growth phase were digested, centrifuged, and grown into 6-well plates. When cells were reached the complete fuse, 10 μl tips were used to make a scratch vertically. Then cells were washed by PBS, and photographed at 0, 24, 48, and 72 h.

Transwell

Cell invasion assay was conducted using Transwell chamber coated with Matrigel (BD Biosciences). Briefly, cells (5×10^4) were re-suspended in a serum-free medium and placed into the top chamber. 600 μl medium containing 10% FBS was put into the lower chamber. Followed by incubation for 48 h at 37°C with 5% CO_2, the cells in the top chamber were wiped and the invaded cells in the lower chamber were fixed with 4% formaldehyde and stained with 0.3% crystal violet. Finally, the number of invaded cells was observed under a microscope at 10 × 10 magnification.

Immunofluorescence

Cells (2.5×10^5) in good condition were fixed with 4% paraformaldehyde at 25°C for 30 min, followed by PBS washing. Then cells were permeated using 0.3% Triton X-100 at 25°C for 10 min, and then sealed with 3% bovine serum albumin after being washed at 37°C for 30 min. Next, cells were incubated with the primary antibodies at 37°C for 1 h. After washing, secondary antibodies were added for 1-hour incubation at 37°C. Finally, DAPI was used for cell counterstaining, and the images were observed using a fluorescence microscope (Olympus) at 100 × 10 magnification.

Western Blot

Total protein was extracted from 1×10^6 cells on six-well plates using RIPA buffer (Beyotime). Every 1 ml lysate was added with 10μg phenylmethylsulfonyl fluoride (PMSF), and the concentration of protein was quantified using BCA working solution (Beyotime). Proteins were electrophoresed in 10% sodium dodecyl sulfate-polyacrylamide gel electrophoresis, and then transferred to polyvinylidene fluoride membranes, followed by sealing in 5% defatted milk. The membrane was incubated with the primary antibodies against matrix metallopeptidase 2 (MMP2; Abcam, 1/1000), matrix metallopeptidase 9 (MMP9; Abcam, 1/1000), E-cadherin (Abcam, 1/1000), N-cadherin (Abcam, 1/1000), WNT2B (Abcam, 1/1000), lymphoid enhancer binding factor 1 (LEF1; Abcam), β-catenin (Abcam), c-MYC (Abcam), cyclin D1 (CCND1; Abcam), cyclin dependent kinase 4 (CDK4; Abcam), Snail (Abcam) and GAPDH (Abcam, 1/1000) for detection of specific proteins. Then the membrane was cultured with HRP-labeled secondary antibody. The protein bands were measured using enhanced chemiluminescence (ECL) western blotting substrate (Millipore). The original images were demonstrated in Supplementary file 2–3.

Subcellular Fractionation

The nuclear and cytoplasmic fractions of 1×10^7 cells were separated using a PARIS kit (Invitrogen) conforming to supplier's protocol. RT-qPCR was used to analyze the expression of LINC00665, U6 and GAPDH, respectively. U6 and GAPDH were regarded as nuclear control and or cytoplasmic control severally.

Fluorescent In Situ Hybridization

Cells (5×10^4) grown on 24-well plates were washed with PBS and fixed with 4% paraformaldehyde. Then cells were treated with 0.3% Triton X-100 for 5 min, followed by incubation with prehybridization buffer at 37°C, and then hybridized with digoxin-labeled probe at 37°C overnight. DAPI was used for nuclear counterstaining, and the images were observed using a fluorescence microscope at 100 × 10 magnification.

MS2-RNA Immunoprecipitation

Maltose-binding protein (MBP)-affinity purification was used to identify the binding relation between miRNAs and LINC00665. On the basis of Steitz laboratory steps, three bacteriophage MS2 coat protein-binding sites were inserted into downstream of LINC00665 using Stratagene Quik Change Site Directed Mutagenesis Kit. Cells (5×10^6) were transfected with MS2-tagged LINC00665 to detect the associations between miRNAs and LINC00665. After 48 h, the cells were subjected to RIP analysis as previously described.[24] The level of miRNAs was measured by RT-qPCR.

RNA Immunoprecipitation

RIP was performed using a Magna RIP RNA-Binding Protein Immunoprecipitation kit (Millipore) based on instructions. Briefly, lysates of 6×10^7 cells were achieved after digesting cells with cell lysis buffer and then hatched with magnetic beads conjugated with negative control anti-immunoglobulin G (IgG) (ab133470, Abcam) or human anti-Argonaute 2 (Ago2) (ab186733, Abcam). The bead-antibody complex was achieved by incubating Protein A/G Agrose with mentioned antibodies at room temperature overnight. The immunoprecipitated RNAs were then extracted and detected by RT-qPCR.

RNA Pull-Down Assay

MiR-1249-5p biotin probe was transfected into 2×10^7 cell lysates, followed by incubation with streptavidin-linked beads at 4°C overnight to form biotin-miRNA-lncRNA or biotin-miRNA-mRNA complex. The purified RNA was analyzed by RT-qPCR.

Luciferase Reporter Assay

We used Cignal Reporter Assay kit to detect the luciferase activity of several pathways including T-cell factor/lymphoid enhancer-binding factor (TCF/LEF), recombination signal binding protein for Jk (RBP-JK), p53, small mothers against decapentaplegic (SMAD), the retinoblastoma protein (pRB)-E2F, nuclear factor-kappaB (NF-κB), MYC proto-oncogene (Myc), hypoxia inducible factor (HIF), serum response element (SRE), and activator protein-1 (AP-1) after LINC00665 knockdown. Besides, the LINC00665 and WNT2B 3′UTR containing the putative miR-1249-5p binding site were severally cloned into the luciferase reporter psiCHECKTM-2 vector (Promega, USA), which named LINC00665-WT and WNT2B 3′UTR-WT. The mutant binding sites of LINC00665 and WNT2B 3′UTR on miR-1249-5p were named LINC00665-MUT and WNT2B 3′UTR-MUT. Then 1×10^4 cells were grown in 96-well plates and co-transfected with these vectors and miR-1249-5p mimics for 48 h. The luciferase activity was assessed using dual luciferase reporter assay kit (Promega). For LINC00665 promoter assay, we constructed the wild-type and mutant-type of luciferase reporter PGL3 vector on LINC00665 promoter at Site 2, and co-transfected into MG-63 or 143B cells under the treatment of lithium chloride (LiCl) for 48 h. The luciferase activity was assessed using luciferase reporter assay kit (Promega).

TOP/FOP-Flash Reporter Assay

TOP/FOP-Flash (Genechem) was co-transfected into cells (5×10^5) along with the transfection of sh-NC, sh-LINC00665 or sh-LINC00665 + pcDNA-WNT2B. The TOP/FOP-Flash values were normalized to the Renilla reniformis (Promega).

Chromatin Immunoprecipitation

The ChIP assay was performed using the EZ-ChIP™ Chromatin immunoprecipitation kit (Millipore). Cells (2×10^7) were incubated using Anti-LEF1 antibody and the purified DNA was analyzed using RT-qPCR.

Statistical Analysis

All experimental data were analyzed using SPSS 21.0 software purchased from International Business Machines Corporation, which were presented as means ± standard deviation of three independent experiments and analyzed using GraphPad PRISM 6 software (GraphPad). Student′s t-test was applied for statistical analysis between two groups and Analysis of Variance was for statistical analysis among three or more groups. $p < 0.05$ was considered as statistically significant.

Results

LINC00665 Facilitates OS Cell Proliferation While Repressing Cell Apoptosis

We severally extracted total RNA from four OS cell lines (U2OS, SAOS-2, MG-63 and 143B) and human fetal osteoblasts (hFOB) and applied RT-qPCR to analyze LINC00665 expression in each cell line. As indicated in Figure 1A, LINC00665 expression was notably higher in four OS cells relative to hFOB. As MG-63 and 143B displayed the highest LINC00665 expression, the two cell lines were selected for transfection with three specific shRNAs targeting LINC00665 in order to inhibit LINC00665 expression. Remarkable reduction in LINC00665 expression was detected after the transfection of sh-LINC00665, especially after sh-LINC00665#1/2 transfection (Figure 1B). Then we assessed the function of LINC00665 in modulating cell viability and found that LINC00665 silence obviously repressed viability of MG-63 and 143B cells (Figure 1C). Besides, we discovered that EdU positive stained cells and colonies were substantially reduced in sh-LINC00665#1 (sh-LINC00665) transfected MG-63 and 143B cells (Figure 1D,E), suggesting that LINC00665 silence reduced OS cell proliferation. Moreover, LINC00665 inhibition was observed to be stimulated when LINC00665 was absent (Figure 1F–G). Similarly, after detecting efficiency of pcDNA-LINC00665 in OS cells (Figure S1A), a series of gain-of-function experiments were conducted correspondingly. Figure S1B evidenced that pcDNA-LINC00665 could enhance OS cell viability, and Figure S1C, D proved pcDNA-LINC00665 could facilitate OS cell proliferation. In addition, after overexpressing LINC00665, OS cell apoptosis was inhibited, as caspase-3 activity was reduced and TUNEL positive cell number declined (Figure S1E, F). All above results revealed that LINC00665 facilitated OS cell proliferation while repressing OS cell apoptosis.

LINC00665 Facilitates OS Cell Malignant Behaviors

Subsequent experiments were implemented to evaluate the changes in OS cell migration, invasion, and epithelial-mesenchymal transition (EMT) in response to LINC00665 silence. We also found that LINC00665 deletion restrained the migratory ability of OS cells (Figure 2A). Besides, the data from Transwell assays disclosed that the LINC00665 deletion decreased the number of invaded cells in OS (Figure 2B). EMT is a biological process which accompanies with cell migration and invasion. Thus, we utilized immunofluorescence staining to detect the intensity of E-cadherin, the epithelium marker, and N-cadherin, the mesenchymal marker in MG-63 and 143B cells after sh-LINC00665 transfection. As indicated in Figure 2C, the intensity of E-cadherin was strengthened while that of N-cadherin was weakened by LINC00665 depletion. Simultaneously levels of EMT-related proteins were quantified, and we confirmed that LINC00665 deletion inhibited the levels of MMP2, MMP9 and N-cadherin while increasing that of E-cadherin (Figure 2D). Then, we tested OS cell migration, invasion and

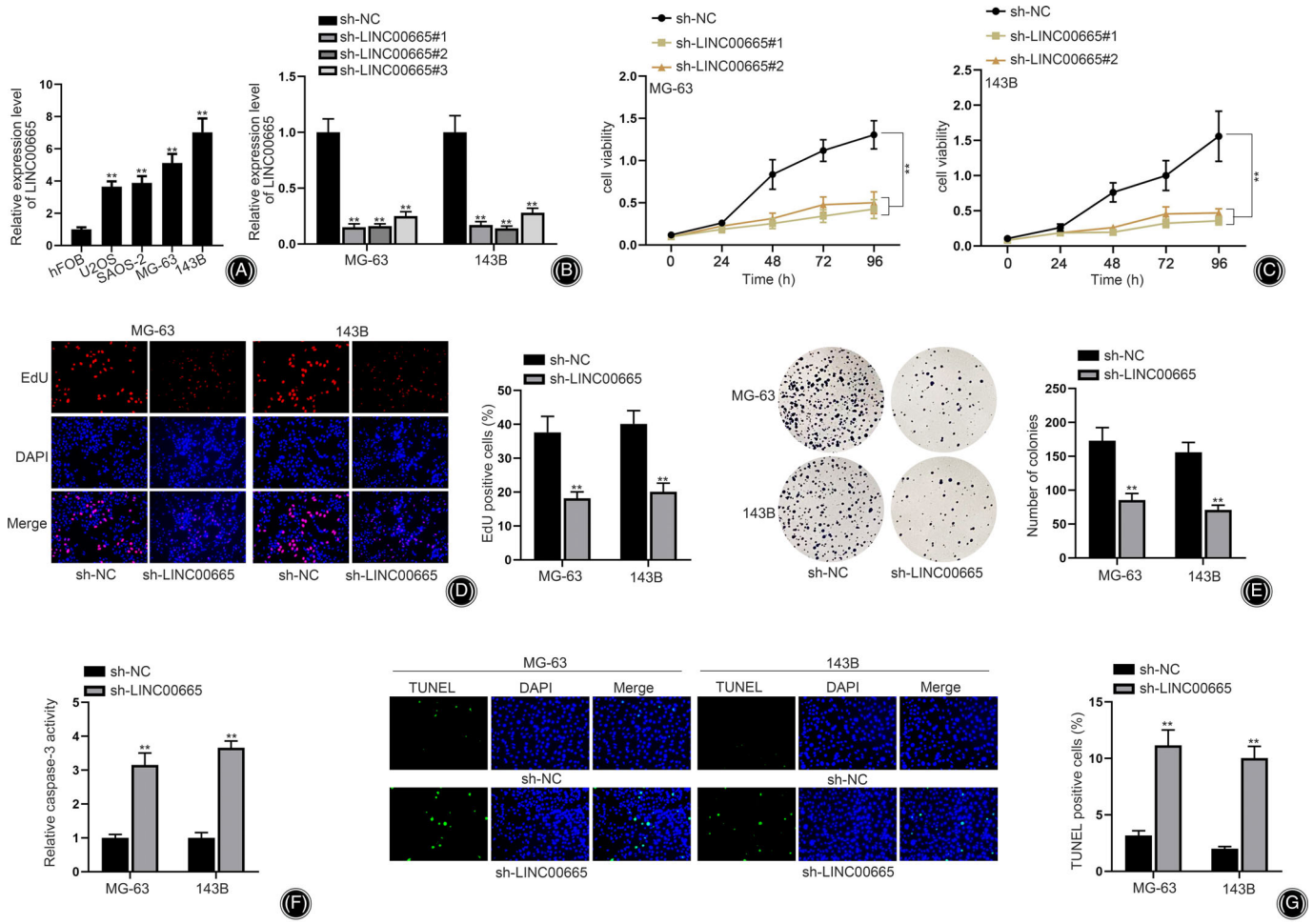

Fig. 1 LINC00665 facilitates OS cell proliferation but represses cell apoptosis. (A) RT-qPCR measured the level of LINC00665 in four OS cell lines and hFOB. (B) RT-qPCR verified the effectiveness of sh-LINC00665#1, sh-LINC00665#2 and sh-LINC00665#3. (C) CCK-8 assays analyzed the influence of LINC00665 silence on OS cell viability. (D, E) EdU and colony formation assays determined the impacts of LINC00665 knockdown on OS cell proliferation. (F, G) Caspase-3 activity and TUNEL assays analyzed the effects of LINC00665 silence on OS cell apoptosis. $^{**}p < 0.01$

EMT processing after overexpressing LINC00665. All results hinted the migration and invasion of OS cells were facilitated due to LINC00665 augment (Figure S1G, H). Moreover, immunofluorescence staining evidenced E-cadherin was attenuated while N-cadherin was increased after LINC00665 overexpression (Figure S1I). WB result confirmed that transfection of pcDNA-LINC00665 could elevate MMP2, MMP9 as well as N-cadherin expression, while decreasing E-cadherin expression (Figure S1J). Taken together, LINC00665 facilitated OS cell malignant behaviors.

LINC00665 Could Bind to miR-1249-5p

LINC00665 has been identified as a ceRNA to act a cancer-promoting role in tumor development,[25] but whether LINC00665 also regulate OS cell behaviors via ceRNA mechanism remains unclear. With the intention to probe into the regulatory mechanism of LINC00665, the cellular location of LINC00665 in OS cells was analyzed. As shown in Figure 3A,B, LINC00665 mainly distributed in the cytoplasm, which implied that LINC00665 might work as a ceRNA. Thus we further used DIANA (http://carolina.imis.athena-innovation.gr/diana_tools/web/) database to predict possible miRNAs that combined with LINC00665, and the top five miRNAs were displayed (Figure 3C). To screen out the most appropriate one, we constructed LINC00665 sequences into MS2-RIP system and transfected them into MG-63 and 143B cells to capture MS2-related complexes through RIP assays. The enrichment of miR-1249-5p was the highest in MS2-LINC00665 groups in comparison with other miRNAs (Figure 3D). Thereby it was confirmed that the binding potential of miR-1249-5p to LINC00665 was the strongest. Subsequently, miR-1249-5p was observed to exhibit lower expression in OS cells compared to hFOB (Figure 3E). Besides, miR-1249-5p level was detected to be

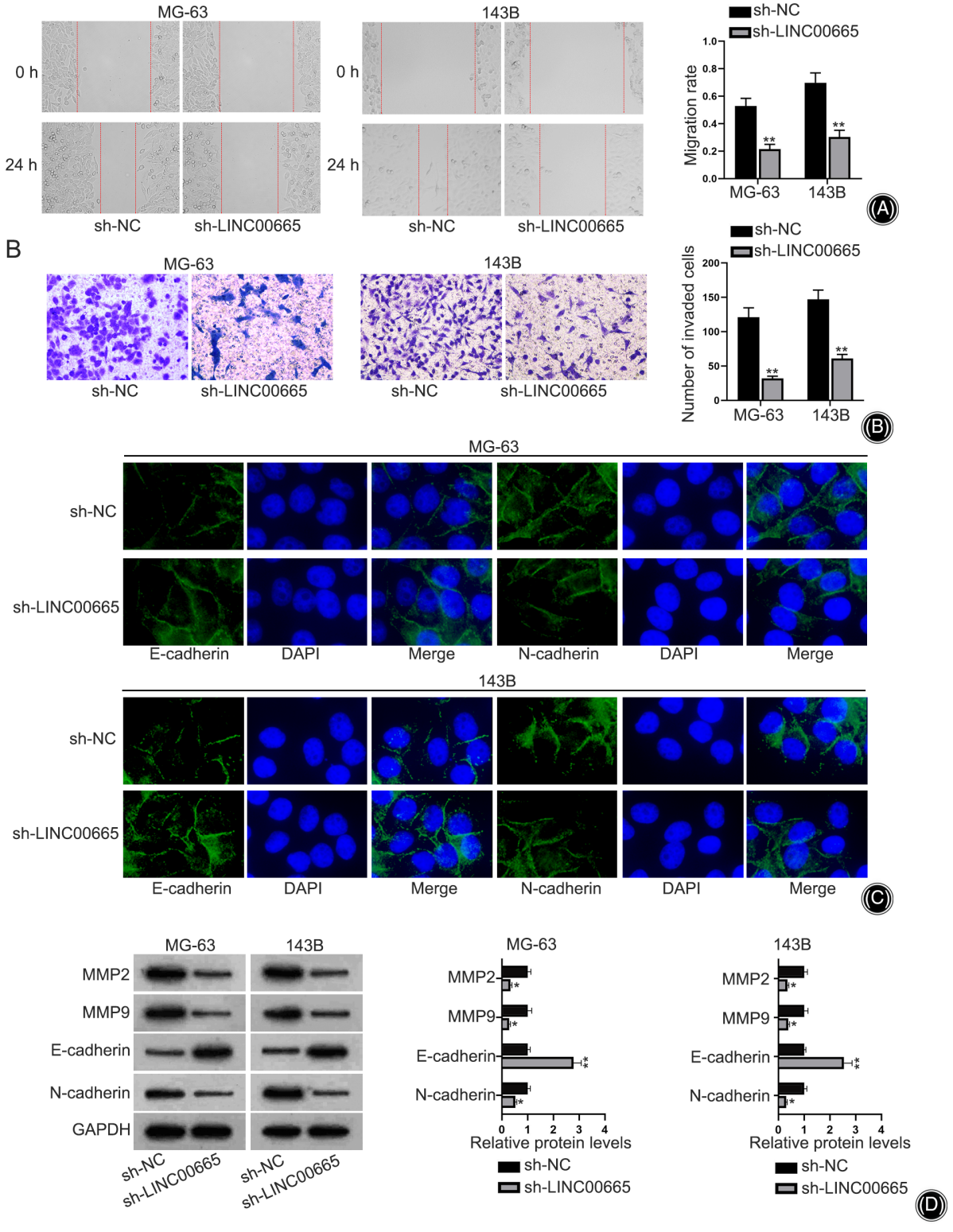

Fig. 2 LINC00665 facilitates OS cell migration, invasion and EMT. (A) Evaluation of the impacts of LINC00665 silence on OS cell migration was achieved via wound healing experiments. (B) Transwell assays detected the function of LINC00665 silence on OS cell invasion. (C) Immunofluorescence staining detected the intensity of E-cadherin and N-cadherin in LINC00665-downregulated cells. (D) Western blot analyzed the impacts of LINC00665 silence on proteins relevant to EMT. *$p < 0.05$, **$p < 0.01$

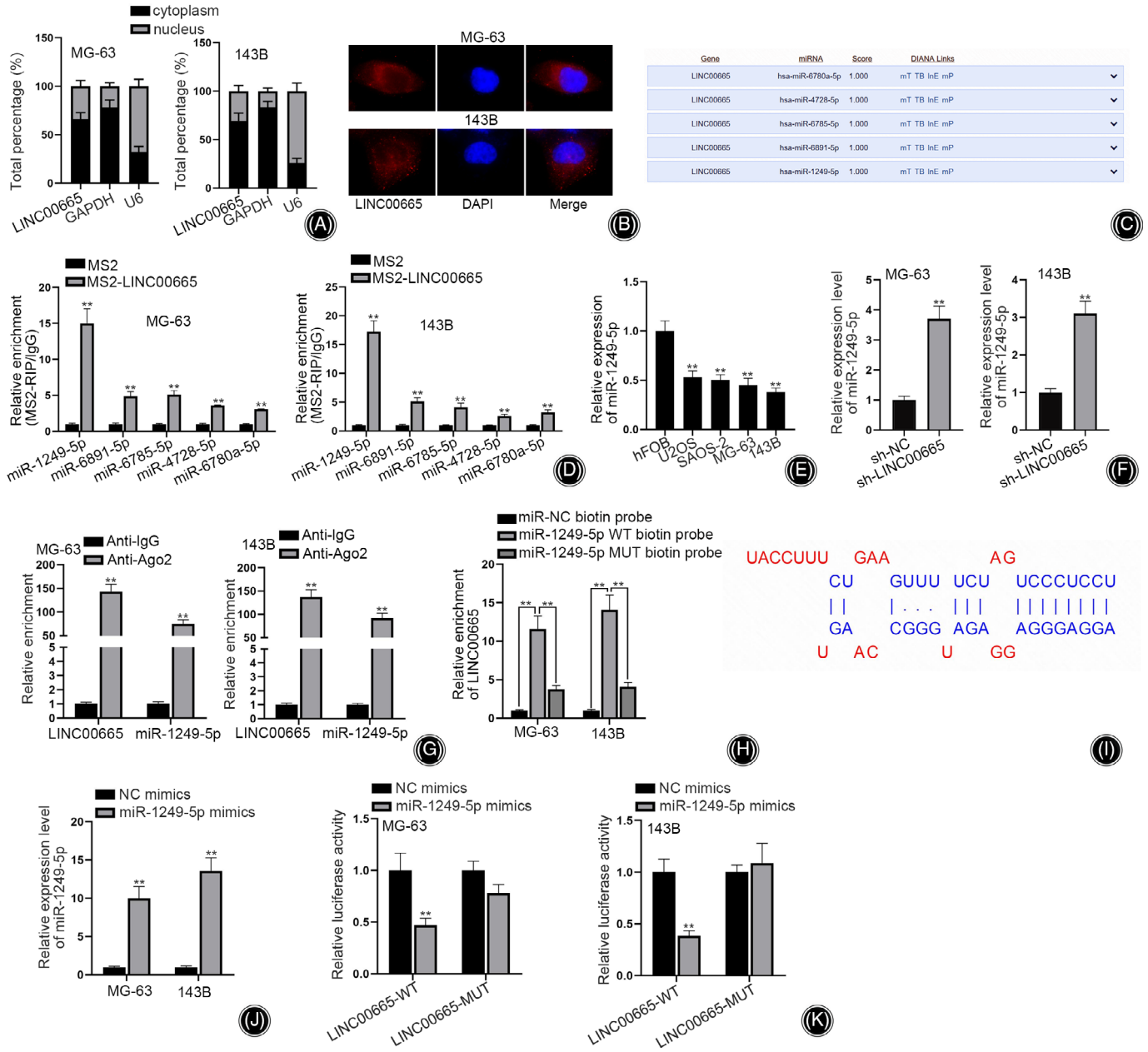

Fig. 3 LINC00665 sequesters miR-1249-5p in OS cells. (A, B) Subcellular fractionation and FISH assays detected LINC00665 accumulation in OS cells. (C) DIANA database predicted the possible miRNAs that combined with LINC00665. (D) The enrichment of five miRNAs in MS2-LINC00665 groups was quantified in MS2-RIP assay, supported by RT-qPCR. (E) RT-qPCR was employed for calculation of miR-1249-5p expression in OS cells. (F) RT-qPCR examined miR-1249-5p expression in OS cells upon LINC00665 depletion. (G) RIP assays detected LINC00665 and miR-1249-5p precipitated in Anti-Ago2. (H) RNA pull-down assays detected LINC00665 level pulled down by miR-1249-5p biotin probe. (I) Potential binding sites between LINC00665 and miR-1249-5p were displayed. (J) RT-qPCR tested the efficacy of miR-1249-5p overexpression in cells. (K) Luciferase reporter assays detected the luciferase activity of LINC00665-WT and LINC00665-MUT in OS cells upon miR-1249-5p up-regulation. $^{**}p < 0.01$

obviously elevated in MG-63 and 143B cells transfected with sh-LINC00665 (Figure 3F). To explore whether LINC00665 and miR-1249-5p were in the same RNA-induced silencing complex (RISC, assembly of small RNA and Ago2), RIP assays were implemented. The enrichment of LINC00665 and miR-1249-5p was both augmented in Ago2 precipitates than that in IgG precipitates (Figure 3G), indicating that LINC00665 functioned as a ceRNA to sequester

miR-1249-5p and regulate miR-1249-5p expression. Moreover, we designed the probe of biotin-labeled miR-1249-5p sequences and treated them into MG-63 and 143B cell lysates to capture miR-1249-5p-combined RNAs. The results revealed that LINC00665 was largely enriched in miR-1249-5p WT biotin probe groups compared to miR-NC biotin probe and miR-1249-5p MUT biotin probe groups (Figure 3H), further suggesting the combination between miR-1249-5p and LINC00665. Subsequently, we projected the putative binding sites between LINC00665 and miR-1249-5p (Figure 3I). We overexpressed miR-1249-5p in OS cells (Figure 3J) and constructed wild-type and mutant-type of LINC00665 luciferase reporters, and then co-transfected them into MG-63 and 143B cells. The data indicated that miR-1249-5p augment dramatically restrained the luciferase activity of LINC00665-WT, while that of LINC00665-MUT was hardly influenced (Figure 3K), reflecting the binding between LINC00665 and miR-1249-5p at the predicted site. Totally, LINC00665 bound to miR-1249-5p in OS cells.

LINC00665 Regulates OS Cell Proliferation and Apoptosis Via Sequestering miR-1249-5p

Furthermore, to clarify the functional influence of LINC00665/miR-1249-5p axis, MG-63 and 143B cells were transfected with sh-NC, sh-LINC00665 or sh-LINC00665 and miR-1249-5p. Then CCK-8 assays were conducted, the result of which confirmed that miR-1249-5p inhibitor could restore the repressed MG-63 and 143B cell viability by LINC00665-shRNA transfection (Figure 4A). Additionally, the results from EdU and colony formation assays indicated reduced proliferation capacity caused by LINC00665 deletion was partially countervailed by miR-1249-5p inhibitor co-transfection (Figure 4B,C). Additionally, through caspase-3 activity and TUNEL analyses, we verified miR-1249-5p inhibitor co-transfection offset the facilitated apoptosis property caused by LINC00665 silence (Figure 4D,E). Collectively, LINC00665 regulated cell proliferation and apoptosis via binding with miR-1249-5p in OS.

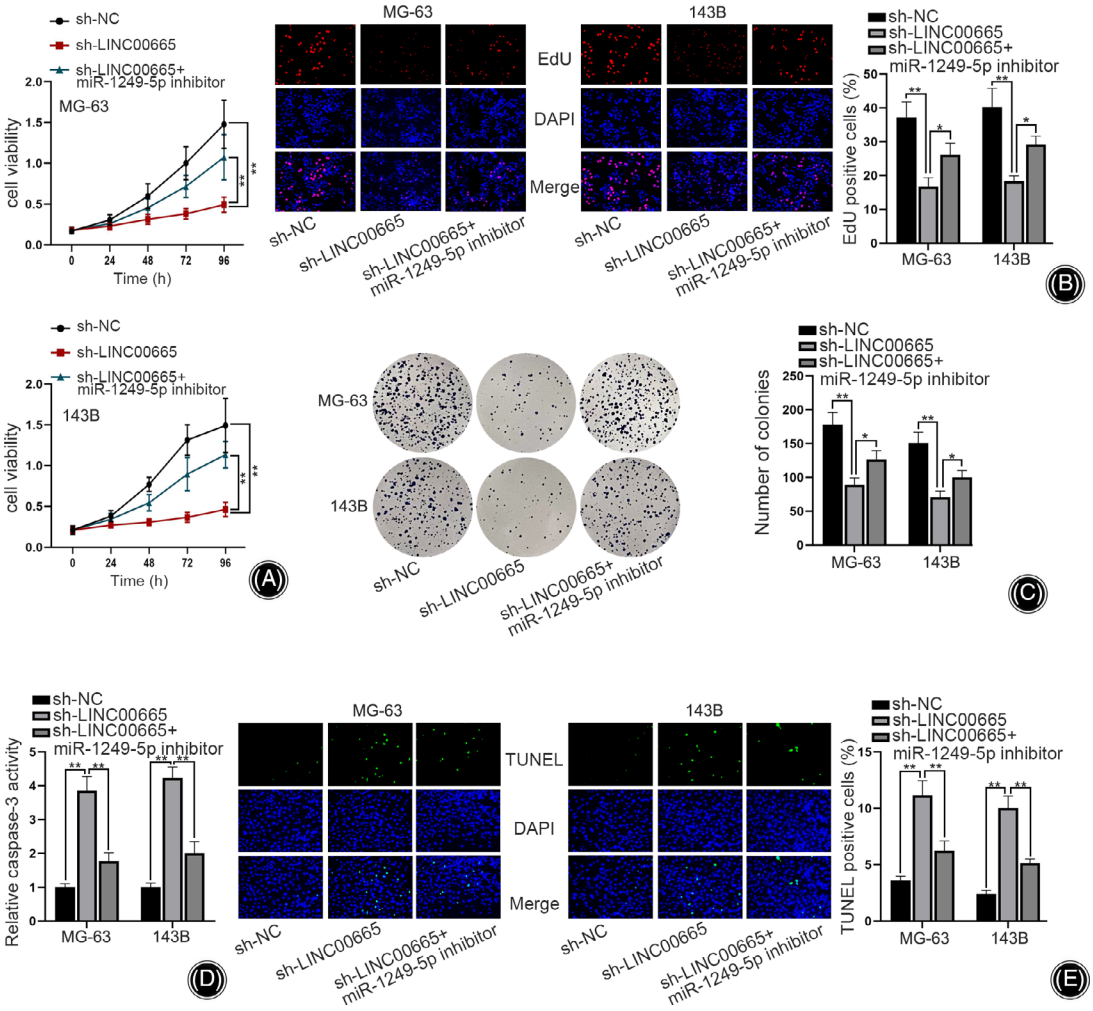

Fig. 4 LINC00665 regulates OS cell proliferation and apoptosis via sequestering miR-1249-5p. (A–C) CCK-8, EdU and colony formation assays evaluated the changes of OS cell proliferation. (D, E) Caspase-3 activity and TUNEL assays detected the apoptosis of OS cells.
*$p < 0.05$, **$p < 0.01$

LINC00665 Facilitates OS Cell Migration, Invasion, and EMT Via Regulating miR-1249-5p

Additionally, it was found in wound healing assays that miR-1249-5p repression recovered the reduced migration ability of sh-LINC00665 transfected OS cells (Figure 5A). Meanwhile, the suppressive invasion potential mediated by LINC00665 absence of OS cells was regained after silence of LINC00665 and miR-1249-5p together (Figure 5B). Moreover, we confirmed that

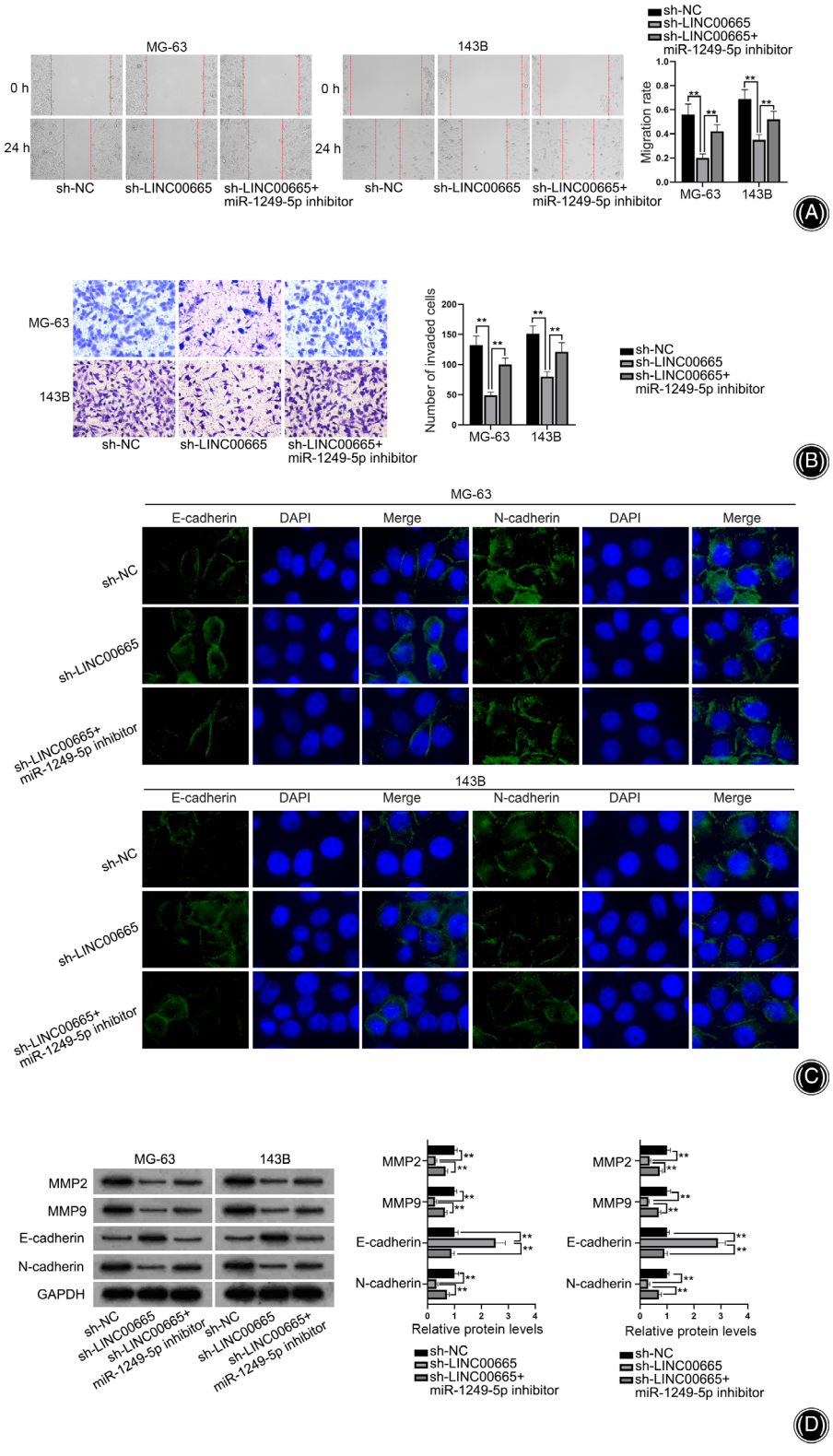

Fig. 5 LINC00665 regulates miR-1249-5p to affect OS cell behaviors. (A) Wound healing assays were implemented for investigation into the migratory ability of cells under different transfection conditions. (B) Transwell assays detected cell invasion in sh-NC group, sh-LINC00665 group and sh-LINC00665 + miR-1249-5p inhibitor group. (C) Immunofluorescence staining detected the intensity of E-cadherin and N-cadherin in cells in different groups. (D) Western blot quantified levels of EMT-related proteins, including MMP2, MMP9, N-cadherin and E-cadherin in different groups. $^{**}p < 0.01$

miR-1249-5p inhibitor neutralized the repressive effects on EMT caused by LINC00665 interference, as miR-1249-5p inhibitor neutralized the increased intensity of E-cadherin and the decreased intensity of N-cadherin in LINC00665-shRNA transfected OS cells (Figure 5C). Likewise, miR-1249-5p inhibitor counteracted the elevated E-cadherin protein level and the inhibited MMP2, MMP9 and N-cadherin protein levels caused by LINC00665 interference (Figure 5D). All above data revealed that LINC00665 facilitated OS cell migration, invasion and EMT via regulating miR-1249-5p.

LINC00665 Binds With miR-1249-5p to Regulate WNT2B Expression

After confirming that LINC00665 regulated miR-1249-5p via ceRNA, we subsequently investigated the downstream of miR-1249-5p. We first explored tumor-related signaling pathways regulated by LINC00665 in OS. We applied cignal reporter assay to figure out the activity of several signaling pathways in OS cells transfected with sh-LINC00665. We found that LINC00665 silence significantly repressed TCF/LEF activity, mirroring that LINC00665 might regulate the Wnt pathway in OS cells (Figure 6A). Then we utilized TargetScan (www.targetscan.org/vert_72/) database to find the possible genes in WNT family that combined with miR-1249-5p, and 10 genes were chosen (Figure 6B). WNT2B was the gene with highest cumulative weighted score of possible combinations with miR-1249-5p. Thus, we selected WNT2B for further analyses. Subsequently, we analyzed WNT2B expression and found that WNT2B presented a higher expression level in OS cells relative to hFOB (Figure 6C). Besides, we noticed that the RNA and protein expressions of WNT2B were evidently lessened in miR-1249-5p mimics transfected cells (Figure 6D). Moreover, we predicted four binding sites between miR-1249-5p and WNT2B 3′UTR via TargetScan website (Figure 6E). To further examine which binding site was the effective one, RNA pull-down assays were designed with miR-1249-5p biotin probe. The data illustrated that WNT2B was significantly enriched in miR-1249-5p biotin probe at Position 1 and Position 2, while had no enrichment in miR-1249-5p biotin probe at Position 3 and Position 4. More importantly, the enrichment of WNT2B in miR-1249-5p WT biotin probe was the highest at Position 1 (Figure 6F). Additionally, we noticed miR-1249-5p up-regulation resulted in a decline of the luciferase activity of WNT2B 3′UTR-WT, and hardly affected that of WNT2B 3′UTR-MUT (Figure 6G). RIP assays confirmed the ceRNA network among LINC00665, miR-1249-5p and WNT2B, as indicated, these three RNAs were substantially enriched in Anti-Ago2 groups (Figure 6H). Finally, we confirmed the reduction in WNT2B expression in sh-LINC00665 transfected OS cells, while such trend was offset by co-transfection of miR-1249-5p inhibitor (Figure 6I). In conclusion, LINC00665 modulated miR-1249-5p to regulate WNT2B expression in OS cells.

LINC00665 Facilitates OS Cell Malignant Phenotypes Via Up-regulating WNT2B

To determine the interaction of LINC00665 and WNT2B on OS cell behaviors, we increased the expression level of WNT2B (Figure 7A) and severally transfected sh-NC, sh-LINC00665 and sh-LINC00665 + pcDNA-WNT2B into MG-63 and 143B cells to perform rescue experiments. The data from CCK-8 assays revealed that WNT2B increase reversed the lessened viability of sh-LINC00665 transfected MG-63 and 143B cells (Figure 7B). Similarly, the inhibited proliferation capacity caused by LINC00665 deletion was restored after co-transfection of pcDNA-WNT2B, as indicated in EdU and colony formation assays (Figure 7C,D). Besides, we found that strengthened apoptotic ability of cells in response to LINC00665 silence was abrogated by WNT2B increment (Figure 7E,F). Moreover, the data from wound healing and Transwell assays uncovered WNT2B increase countervailed the repressive impact of LINC00665 knockdown on OS cell migration and invasion (Figure 7G,H). Additionally, the inhibited EMT process in LINC00665 silenced cells were rescued by co-transfection of pcDNA-WNT2B (Figure 7I,J). Notably, we also utilized TOP/FOP-flash reporter assays to find that knockdown of LINC00665 obviously inhibited the activity of the Wnt pathway, while co-transfection of pcDNA-WNT2B offset this effect caused by LINC00665 silence (Figure S2A). In parallel, western blot was applied to testify the impacts of LINC00665 and WNT2B on the key genes and downstream genes in the Wnt pathway. As was demonstrated in Figure S2B, WNT2B, β-catenin, LEF1, c-MYC, CCND1, CDK4, MMP2, and Snail expressions were obviously reduced when LINC00665 was knocked down, while co-transfection of pcDNA-WNT2B offset this effect. In short, LINC00665 facilitated malignant behaviors of OS cells and the Wnt pathway via up-regulating WNT2B.

Wnt Pathway Enhances LINC00665 Expression

Previous study has demonstrated that a positive feedback loop between lncRNA and the Wnt signaling in cancer development.[26] Herein, we also guessed whether LINC00665 up-regulation in OS cells was related to the Wnt pathway. We treated MG-63 and 143B cells with LiCl (Wnt pathway activator) and found that LINC00665 expression was evidently augmented in LiCl groups in comparison to dimethyl sulfoxide (DMSO) groups (Figure S3A). To further verify that the Wnt pathway modulated the expression of LINC00665 transcriptionally, the luciferase activity of LINC00665 promoter under the treatment of LiCl was analyzed. It was implied that the luciferase activity of LINC00665 promoter was obviously elevated upon LiCl treatment (Figure S3B). Through JASPAR (http://jaspar.genereg.net/) database, we found the DNA motif sequences of the TCF/LEF transcription complex and the two possible binding sites of TCF/LEF transcription complex on LINC00665 promoter (Figure S3C, D). Furthermore, we conducted ChIP assays to validate that LINC00665 was highly

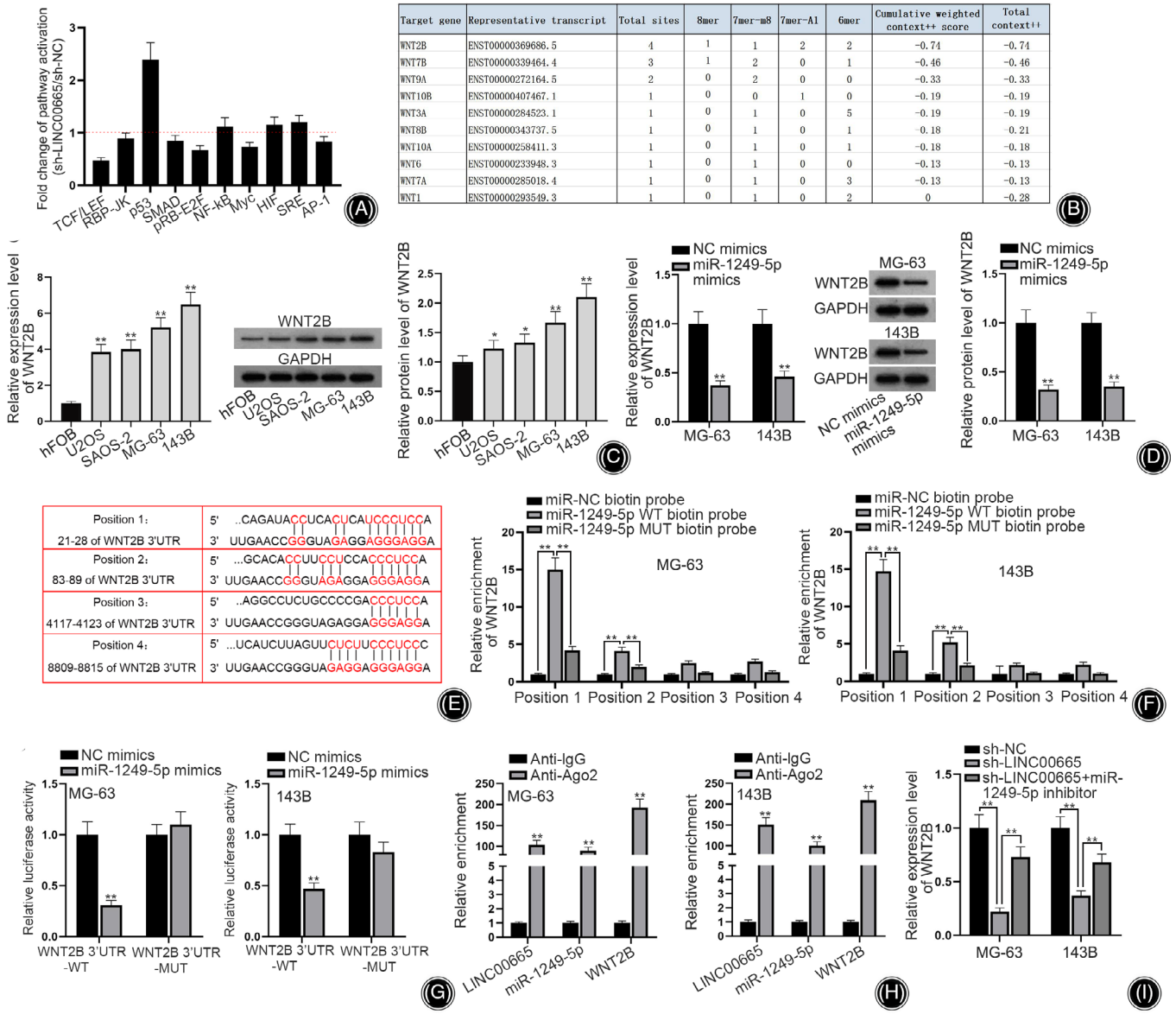

Fig. 6 LINC00665 binds with miR-1249-5p to regulate WNT2B expression. (A) Cignal reporter assays detected the activity of several signaling pathways in OS cells transfected with sh-LINC00665. (B) TargetScan database predicted the possible genes in WNT family that combined with miR-1249-5p. (C) RT-qPCR and western blot examined WNT2B expression in OS cells and hFOB. (D) RT-qPCR and western blot analyzed RNA and protein levels of WNT2B in miR-1249-5p-upregulated cells. (E) Four binding sites between miR-1249-5p and WNT2B 3′UTR were projected using TargetScan website. (F) RNA pull-down assays assessed the potential binding between WNT2B and miR-1249-5p at four positions, respectively. (G) Luciferase reporter assays detected the luciferase activity of WNT2B 3′UTR-WT and WNT2B 3′UTR-MUT in MG-63 and 143B cells co-transfected with miR-1249-5p mimics. (H) In RIP assays, the enrichment of LINC00665, miR-1249-5p and WNT2B in Anti-Ago2 groups was measured. (I) Detection of WNT2B expression in cells transfected with different plasmids was completed with RT-qPCR. $*p < 0.05$, $**p < 0.01$

enriched in Anti-LEF1 groups at Site 2 (Figure S3E), and we constructed the luciferase reporter vector with wild-type and mutant-type of LINC00665 promoter at Site 2, and co-transfected these vectors into MG-63 and 143B cells under the treatment of LiCl. The luciferase activity of LINC00665 promoter-WT was obviously enhanced while that of LINC00665 promoter-MUT was not changed after LiCl treatment (Figure S3F). All above data indicated that the Wnt pathway enhanced LINC00665 expression.

Discussion

In brief, this study uncovered that LINC00665 had a high expression and exerted a cancer-promoting role in OS cells. Mechanistically, LINC00665 combined with

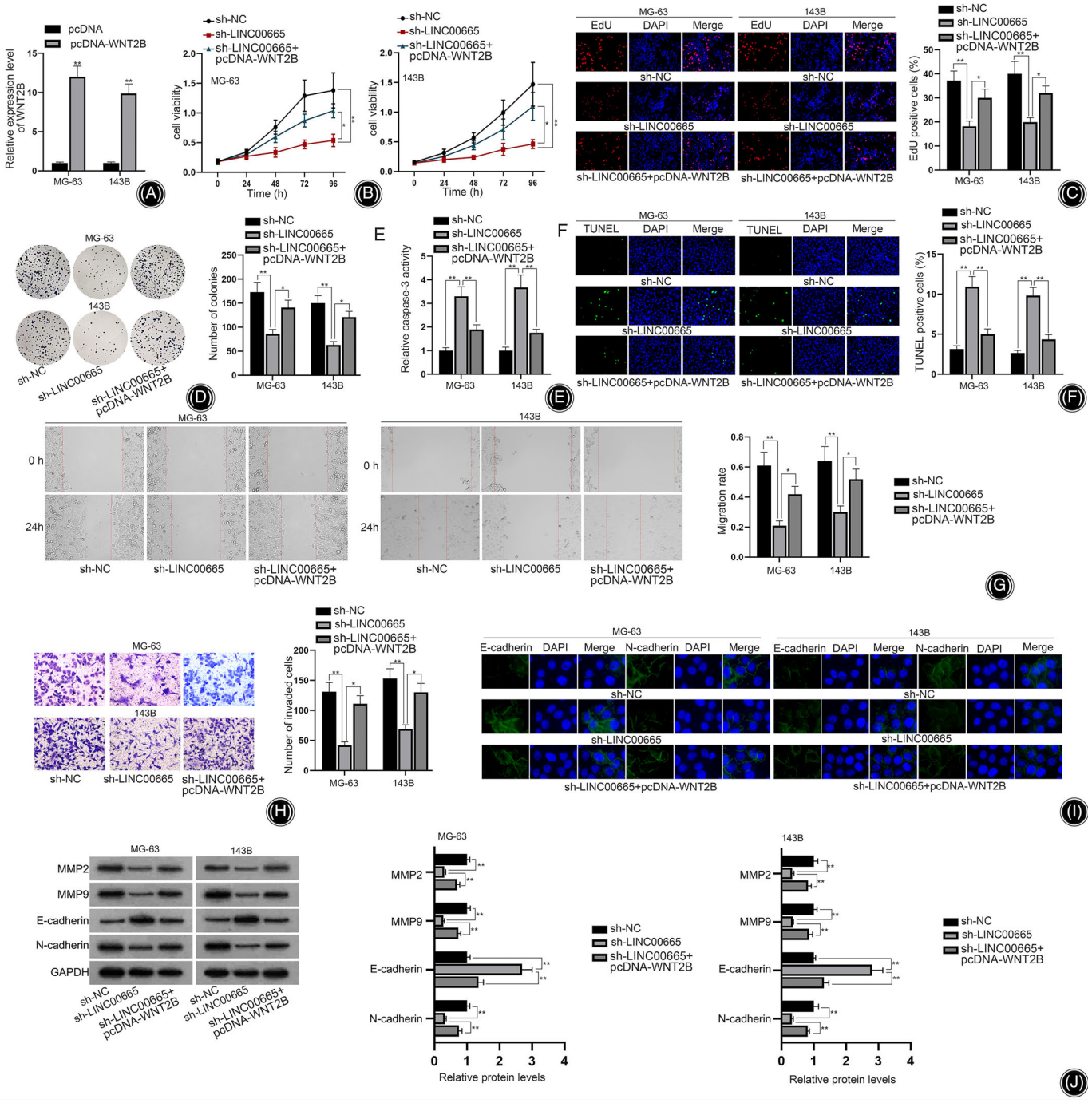

Fig. 7 LINC00665 facilitates malignant behaviors of OS cells via up-regulating WNT2B. (A) RT-qPCR tested the overexpression efficacy of pcDNA-WNT2B. (B–D) CCK-8, EdU and colony formation assays evaluated the proliferation ability of cells in different groups. (E, F) Caspase-3 activity and TUNEL assays detected the cell apoptosis upon transfection of sh-NC, sh-LINC00665 or sh-LINC00665 + pcDNA-WNT2B. (G) Wound healing assays assessed the migratory capability of cells with transfection of sh-NC, sh-LINC00665 and sh-LINC00665 + pcDNA-WNT2B. (H) Transwell assays detected the invasion ability of cells. (I) Immunofluorescence staining detected the intensity of E-cadherin and N-cadherin in cells. (J) EMT-related proteins in OS cells were quantified via western blot. $*p < 0.05$, $**p < 0.01$

miR-1249-5p and inhibited its expression, accordingly up-regulating WNT2B, thus affecting Wnt pathway. Wnt pathway was also verified to increase LINC00665 expression. Additionally, miR-1249-5p inhibition or WNT2B increment was observed to abrogate the suppressive impact of LINC00665 depletion on malignant phenotype of OS cells.

LINC00665 Exerted Promoting Effect on the Malignant Behaviors of OS Cells

Accumulating evidence has exposed that lncRNAs are important regulators of cancers. LINC00665 is elevated in hepatocellular carcinoma and knockdown of LINC00665 represses hepatocellular carcinoma cell viability while increasing cell apoptosis and autophagy.[27] LINC00665 has aberrantly high expression in breast cancer and has been confirmed to facilitate cell migration and invasion.[28] Nevertheless, the expression and role of LINC00665 in OS remain quite obscure. In this study, LINC00665 expression in OS cells was ascertained to be high. LINC00665 deletion obviously repressed OS cell proliferation, migration, and EMT, while increasing cell apoptosis, which was opposite to the results caused by LINC00665 overexpression, suggesting the tumor-promoting role of LINC00665 in OS cells.

MiR-1249-5p Bound with LINC00665 and Functioned as a Cancer Suppressor in OS Cells

Existing study has disclosed that LINC00665 strengthens the capacities of proliferation, migration, and invasion of colorectal cancer cells by sequestering miR-9-5p to regulate ATF1 expression.[29] This evidence implies the ceRNA regulation of LINC00665 in cancers, which means that LINC00665 can directly bind to miRNA and regulate the expression of the downstream target gene. In line with this evidence, our study found that LINC00665 could bind with miR-1249-5p and thereby inhibit miR-1249-5p expression. Previous publication has reported that miR-1249-5p promotes the progression of colon cancer.[30] Herein, we clarified that miR-1249-5p was low expressed in OS cells. Moreover, rescue experiments were conducted, and it was validated that miR-1249-5p inhibitor could reverse the suppressive effects on OS cell malignant behaviors caused by LINC00665 silence, suggesting miR-1249-5p played as a tumor suppressor in OS cells.

LINC00665 Promoted Malignant Phenotype of OS Cells and Activated Wnt Pathway Via Sequestering miR-1249-5p to Up-regulate WNT2B

LINC00665 has been recognized to exert oncogenic influence via sponging miR-98 to regulate AKR1B10 expression and thereby activates ERK signaling in lung adenocarcinoma.[31] In our study, LINC00665 silence was confirmed to inhibit the activity of TCF/LEF. As we know, the activation of the β-catenin-mediated Wnt signaling is the process of cytoplasmic β-catenin transferring to the nucleus. Nuclear β-catenin binds to proteins of the TCF/LEF family, which function as transcription factors, thus activating the transcription of Wnt target genes.[32] The notion that lncRNAs activate the Wnt signaling to facilitate the development of OS has been widely reported.[33,34] Moreover, our study found that one of the Wnt family genes, namely WNT2B, was targeted by miR-1249-5p. WNT2B is a typical oncogene and has been reported to promote cell proliferation, migration, invasion, and EMT in cancers. Specifically, significant up-regulation of WNT2B has been associated with exacerbated nasopharyngeal carcinoma cell migration and invasion,[35–37] while WNT2B negatively regulated by miR-577 has also been validated to facilitate malignant behaviors of non-small cell lung cancer cells.[32] Moreover, WNT2B targeted by lncRNA SNHG7/miR-324-3p has also been confirmed as a promoting factor leading to enhanced prostate cancer cell migratory and invasive ability via inducing EMT.[33] Of note, WNT2B has been discovered as an oncogene in OS cells.[38] Herein, we also figured out that WNT2B, negatively regulated by miR-1249-5p, exhibited a high expression level in OS cells. Rescue experiments further validated that WNT2B up-regulation could rescue the inhibited malignant behaviors of OS cells induced by LINC00665 depletion, suggesting LINC00665 promoted malignant behaviors of OS cells and the Wnt pathway via up-regulating WNT2B expression.

Wnt Pathway Activation Enhanced LINC00665 Expression

Notably, our study also found that the Wnt pathway could activate LINC00665 up-regulation at the transcription level, which formed a positive feedback loop of LINC00665 and the Wnt pathway.

Strengths and Limitations

This study was the first to put forward a positive loop involving LINC00665/miR-1249-5p/WNT2B and Wnt signaling pathway in OS cells. However, there were still some limitations to be dealt with before confirming the function of the indicated loop in OS progression, Specifically, clinical samples should be included to detect the expression of LINC00665, and xenografts should be constructed to analyze the validity of the loop in vivo.

Conclusion

TCF/LEF transcription complex induced the up-regulation of LINC00665 and LINC00665 promoted OS cell growth. Mechanistically, LINC00665 functioned as a ceRNA to modulate miR-1249-5p and thereby up-regulate WNT2B to enhance the Wnt pathway and the expression of downstream genes, which formed a positive feedback loop. All findings implied that LINC00665 might serve as a novel biomarker in OS treatment.

Acknowledgements

We appreciate the support of laboratory.

Authors' Contributions

Yingzi Zhang, Lin Bo, and Xiao Zhang co-designed the study and prepared all the figures. Huajian Shan and

Xiang Gao took charge of the material collecting and performed the experiment. Yingzi Zhang, Lin Bo, Xiao Zhang, and Jinyu Bai analyzed all the data. Guangsi Shen and Xiaozhong Zhou wrote the study. All authors have read and approved the final manuscript.

Conflict of Interest

The authors declare that there is no conflict of interest.

Ethics Approval and Consent to Participate

Our study did not require an ethical board approval because it did not contain human or animal trials.

Funding Information

This work was supported by the grants from National Natural Science Foundation of China (81902207, 81873995 and 81802194), Key Laboratory of Spinal Cord Injury Repair of Suzhou (SZS201807), the Suzhou Young Science and Technology Project (KJXW2018012), Suzhou Industrial Technology Innovation Project (People's Livelihood Science and Technology-Basic Research on Medical and Health Application, SYSD2016165), Natural Science Foundation of Jiangsu Province (BK20170957).

Data Availability Statement

Not applicable.

Supporting Information

Additional Supporting Information may be found in the online version of this article on the publisher's web-site:

FIGURE S1 LINC00665 overexpression exacerbates the malignant behaviors of OS cells. (A) RT-qPCR verified the efficiency of pcDNA-LINC00665. (B) CCK-8 assays assessed the effect of LINC00665 overexpression on OS cell viability. (C, D) EdU and colony formation assays explored the impacts of LINC00665 upregulation on OS cell proliferation. (E, F) Caspase-3 activity and TUNEL assays measured the OS cell apoptosis after LINC00665 overexpression. (G) Wound healing assays evaluated OS cell migration after upregulating LINC00665. (H) Transwell assays detected the effect of LINC00665 augment on cell invasion in OS. (I) Immunofluorescence staining measured the intensity of E-cadherin and N-cadherin in OS cells transfected with pcDNA-LINC00665. (J) After overexpressing LINC00665, levels of four proteins were calculated via western blot. $^{**}p < 0.01$

FIGURE S2 LINC00665 activates Wnt pathway via upregulating WNT2B. (A) TOP/FOP-flash reporter assays assessed the impacts of LINC00665 and WNT2B on the activity of the Wnt pathway. (B) Western blot measured the impacts of LINC00665 and WNT2B on key and downstream protein levels in the Wnt pathway. $^{**}p < 0.01$

FIGURE S3 Wnt pathway enhances LINC00665 expression. (A) RT-qPCR detected LINC00665 expression in cells under LiCl treatment. (B) Luciferase reporter assays detected the luciferase activity of LINC00665 promoter in cells treated with LiCl. (C, D) JASPAR database predicted the DNA motif sequences of the TCF/LEF transcription complex and the two possible binding sites of TCF/LEF transcription complex on LINC00665 promoter. (E) ChIP assays detected the enrichment of LINC00665 promoter in Anti-LEF1 at Site 1 and Site 2. (F) Luciferase reporter assays detected the luciferase activity of LINC00665 promoter-WT and LINC00665 promoter-MUT at Site 2 in MG-63 and 143B cells treated with LiCl. $^{**}p < 0.01$

References

1. Ritter J, Bielack SS. Osteosarcoma. Ann Oncol. 2010;21(Suppl 7): vii320–5.
2. Lee RJ, Arshi A, Schwartz HC, Christensen RE. Characteristics and prognostic factors of osteosarcoma of the jaws: a retrospective cohort study. JAMA Otolaryngol Head Neck Surg. 2015;141(5):470–7.
3. Corre I, Verrecchia F, Crenn V, Redini F, Trichet V. The osteosarcoma microenvironment: a complex but targetable ecosystem. Cell. 2020;9(4).
4. Stitzlein RN, Wojcik J, Sebro RA, Balamuth NJ, Weber KL. Team approach: osteosarcoma of the distal part of the femur in adolescents. JBJS reviews. 2017; 5(12):e5.
5. Guo J, Reddick WE, Glass JO, Ji Q, Billups CA, Wu J, et al. Dynamic contrast-enhanced magnetic resonance imaging as a prognostic factor in predicting event-free and overall survival in pediatric patients with osteosarcoma. Cancer. 2012; 118(15):3776–85.
6. Kager L, Tamamyan G, Bielack S. Novel insights and therapeutic interventions for pediatric osteosarcoma. Fut Oncol (London, England). 2017;13(4):357–68.
7. Lu KH, Lin RC, Yang JS, Yang WE, Reiter RJ, Yang SF. Molecular and cellular mechanisms of melatonin in osteosarcoma. Cell. 2019;8(12).
8. Zheng C, Tang F, Min L, Hornicek F, Duan Z, Tu C. PTEN in osteosarcoma: recent advances and the therapeutic potential. Biochim Biophys Acta Rev Cancer. 2020;1874(2):188405.
9. Zhou C, Zhang Z, Zhu X, Qian G, Zhou Y, Sun Y, et al. N6-Methyladenosine modification of the TRIM7 positively regulates tumorigenesis and chemoresistance in osteosarcoma through ubiquitination of BRMS1. EBioMedicine. 2020;59:102955.
10. Liu X, Hao L, Li D, Zhu L, Hu S. Long non-coding RNAs and their biological roles in plants. Genomics Proteomics Bioinformatics. 2015;13(3):137–47.
11. Shen B, Zhou N, Hu T, Zhao W, Wu D, Wang S. LncRNA MEG3 negatively modified osteosarcoma development through regulation of miR-361-5p and FoxM1. J Cell Physiol. 2019;234(8):13464–80.
12. Zhao J, Ma ST. Downregulation of lncRNA H19 inhibits migration and invasion of human osteosarcoma through the NF-κB pathway. Mol Med Rep. 2018;17(5):7388–94.
13. Wang Y, Kong D. LncRNA GAS5 represses osteosarcoma cells growth and metastasis via sponging miR-203a. Cell Physiol Biochem. 2018;45(2):844–55.
14. Chen W, Yu Z, Huang W, Yang Y, Wang F, Huang H. LncRNA LINC00665 promotes prostate cancer progression via miR-1224-5p/SND1 axis. Onco Targets Ther. 2020;13:2527–35.
15. Ji W, Diao YL, Qiu YR, Ge J, Cao XC, Yu Y. LINC00665 promotes breast cancer progression through regulation of the miR-379-5p/LIN28B axis. Cell Death Dis. 2020;11(1):16.
16. Wang C, Li M, Wang S, Jiang Z, Liu Y. LINC00665 promotes the progression of multiple myeloma by adsorbing miR-214-3p and positively regulating the expression of PSMD10 and ASF1B. Onco Targets Ther. 2020; 13:6511–22.
17. Ding J, Zhao J, Huan L, Liu Y, Qiao Y, Wang Z, et al. Inflammation-induced LINC00665 increases the malignancy through activating PKR/NF-κB pathway in hepatocellular carcinoma. Hepatology (Baltimore, Md). 2020;72: 1666–81.
18. Nusse R, Clevers H. Wnt/β-catenin signaling, disease, and emerging therapeutic modalities. Cell. 2017;169(6):985–99.
19. Clevers H, Loh KM, Nusse R. Stem cell signaling. An integral program for tissue renewal and regeneration: Wnt signaling and stem cell control. Science (New York, NY). 2014;346(6205):1248012.

20. Zhang H, Yan J, Lang X, Zhuang Y. Expression of circ_001569 is upregulated in osteosarcoma and promotes cell proliferation and cisplatin resistance by activating the Wnt/β-catenin signaling pathway. Oncol Lett. 2018;16(5):5856–62.
21. Suh HN, Kim MJ, Jung YS, Lien EM, Jun S, Park JI. Quiescence exit of tert(+) stem cells by Wnt/β-catenin is indispensable for intestinal regeneration. Cell Rep. 2017;21(9):2571–84.
22. Chen M, Zhou L, Liao Z, Ye X, Xuan X, Gu B, et al. Sevoflurane inhibited osteosarcoma cell proliferation and invasion via targeting miR-203/WNT2B/Wnt/β-catenin axis. Cancer Manag Res. 2019;11:9505–15.
23. Chen W, Zhao W, Zhang L, Wang L, Wang J, Wan Z, et al. MALAT1-miR-101-SOX9 feedback loop modulates the chemo-resistance of lung cancer cell to DDP via Wnt signaling pathway. Oncotarget. 2017;8(55):94317–29.
24. Luan W, Li L, Shi Y, Bu X, Xia Y, Wang J, et al. Long non-coding RNA MALAT1 acts as a competing endogenous RNA to promote malignant melanoma growth and metastasis by sponging miR-22. Oncotarget. 2016;7(39):63901–12.
25. Qi H, Xiao Z, Wang Y. Long non-coding RNA LINC00665 gastric cancer tumorigenesis by regulation miR-149-3p/RNF2 axis. Onco Targets Ther. 2019;12: 6981–90.
26. Yue B, Liu C, Sun H, Liu M, Song C, Cui R, et al. A positive feed-forward loop between LncRNA-CYTOR and Wnt/β-catenin signaling promotes metastasis of colon cancer. Mol Ther. 2018;26(5):1287–98.
27. Shan Y, Li P. Long intergenic non-protein coding RNA 665 regulates viability, apoptosis, and autophagy via the MiR-186-5p/MAP4K3 axis in hepatocellular carcinoma. Yonsei Med J. 2019;60(9):842–53.
28. Zhou JL, Zou L, Zhu T. Long non-coding RNA LINC00665 promotes metastasis of breast cancer cells by triggering EMT. Eur Rev Med Pharmacol Sci. 2020;24(6):3097–104.
29. Zhao X, Weng W, Long Y, Pan W, Li Z, Sun F. LINC00665/miR-9-5p/ATF1 is a novel axis involved in the progression of colorectal cancer. Hum Cell. 2020;33: 1142–54.
30. Yoshii S, Hayashi Y, Iijima H, Inoue T, Kimura K, Sakatani A, et al. Exosomal microRNAs derived from colon cancer cells promote tumor progression by suppressing fibroblast TP53 expression. Cancer Sci. 2019;110(8):2396–407.
31. Cong Z, Diao Y, Xu Y, Li X, Jiang Z, Shao C, et al. Long non-coding RNA linc00665 promotes lung adenocarcinoma progression and functions as ceRNA to regulate AKR1B10-ERK signaling by sponging miR-98. Cell Death Dis. 2019; 10(2):84.
32. Doumpas N, Lampart F, Robinson MD, Lentini A, Nestor CE, Cantù C, et al. TCF/LEF dependent and independent transcriptional regulation of Wnt/β-catenin target genes. EMBO J. 2019;38(2).
33. Dai J, Xu LJ, Han GD, Jiang HT, Sun HL, Zhu GT, et al. Down-regulation of long non-coding RNA ITGB2-AS1 inhibits osteosarcoma proliferation and metastasis by repressing Wnt/β-catenin signalling and predicts favourable prognosis. Artif Cells Nanomed Biotechnol. 2018;46(sup3):S783–s90.
34. Keremu A, Maimaiti X, Aimaiti A, Yushan M, Alike Y, Yilihamu Y, et al. NRSN2 promotes osteosarcoma cell proliferation and growth through PI3K/Akt/MTOR and Wnt/β-catenin signaling. Am J Cancer Res. 2017;7(3):565–73.
35. Liu C, Li G, Yang N, Su Z, Zhang S, Deng T, et al. miR-324-3p suppresses migration and invasion by targeting WNT2B in nasopharyngeal carcinoma. Cancer Cell Int. 2017;17:2.
36. Wang B, Sun L, Li J, Jiang R. miR-577 suppresses cell proliferation and epithelial-mesenchymal transition by regulating the WNT2B mediated Wnt/β-catenin pathway in non-small cell lung cancer. Mol Med Rep. 2018;18(3):2753–61.
37. Han Y, Hu H, Zhou J. Knockdown of LncRNA SNHG7 inhibited epithelial-mesenchymal transition in prostate cancer though miR-324-3p/WNT2B axis in vitro. Pathol Res Pract. 2019;215(10):152537.
38. Jiang Z, Jiang C, Fang J. Up-regulated lnc-SNHG1 contributes to osteosarcoma progression through sequestration of miR-577 and activation of WNT2B/Wnt/β-catenin pathway. Biochem Biophys Res Commun. 2018;495(1): 238–45.